

A GENERAL ALGORITHM FOR EVALUATING DOMAIN INTEGRALS IN 2D BOUNDARY ELEMENT METHOD FOR TRANSIENT HEAT CONDUCTION

YUNQIAO DONG, JIANMING ZHANG*, GUIZHONG XIE, CHENJUN LU, YUAN LI, XU HAN, and
GUANGYAO LI

*State Key Laboratory of Advanced Design and Manufacturing for Vehicle Body,
Hunan University, Changsha 410082, China*

*zhangjm@hnu.edu.cn

Received 5 November 2013
Accepted 28 September 2014

A time-dependent boundary integral equation method named as pseudo-initial condition method is widely used to solve the transient heat conduction problems. Accurate evaluation of the domain integrals in the pseudo-initial condition formulation is of crucial importance for its successful implementation. As the time-dependent kernel in the domain integral is close to singular when small time step is used, a straightforward computation using Gaussian quadrature may produce large errors, and thus lead to instability of the analysis. To improve the computational accuracy of the domain integral, a coordinate transformation coupled with a domain cell subdivision technique is presented in this paper for 2D boundary element method. The coordinate transformation is denoted as (α, β) transformation, while the cell subdivision technique considers the position of the source point, the shape of the integration cell and the relations between the size of the cell and the time step. With the cell subdivision technique, more Gaussian points are shifted towards the source point, thus more accurate results can be obtained. Numerical examples have demonstrated the accuracy and efficiency of the proposed method.

Keywords: Domain integrals; transient heat conduction; boundary element method; cell subdivision technique.

1. Introduction

The transient heat conduction problem widely appears in engineering problem. There are many numerical methods for this problem such as the finite element method (FEM) [Xue *et al.* (2013); Hamza-Cherif *et al.* (2007)] and the boundary element method (BEM) [Brebbia *et al.* (1984); Sutradhar *et al.* (2002); Hill and Farris (1995); Ibáñez and Power (2000); Gupta *et al.* (1995); Ma *et al.* (2008); Wang *et al.* (2005); Zhou *et al.* (2013); Lesnic (2004); Mukherjee and Liu (2013); Zhuang *et al.* (2013); Dargush and Banerjee (1991); Guo *et al.* (2013)]. The BEM is a very attractive method to analyze the transient heat conduction problem. The implementation of BEM based on time-dependent fundamental solution for transient heat conduction problem can be classified into two kinds: the time convolution method and the pseudo-initial condition method. In the time convolution method, temperature and flux at each step are computed through a convolution of temperature and flux on the boundary at previous steps. If the initial

temperature and the heat generation are omitted, the time convolution method leads to a pure boundary method. However, as indicated in [Ibáñez and Power (2000); Gupta *et al.* (1995); Ma *et al.* (2008); Wang *et al.* (2005); Zhou *et al.* (2013);], the time convolution method suffers from the time-consuming convolution especially in the case that a long time history is concerned. Compared with the time convolution method, no time consuming convolution is required in the pseudo-initial condition method. Therefore, the pseudo-initial condition method is more widely used than the time convolution method in engineering problem. When using the pseudo-initial condition method, the temperature computed in the previous step is considered as the initial condition in current step. Thus, the domain integral of this pseudo-initial condition is required in this method.

Although the domain integrals are actually regular in nature, they can't be evaluated accurately and efficiently by the standard Gaussian quadrature. This is because as the time step approaches zero, the integrand in the domain integral (the time-dependent fundamental solution) is close to singular when the source point is on the integration cell. The difficulty of numerically integrating a function with such behavior can introduce numerical unstable problems into the solution, as reported in [Sharp (1986); Peirce *et al.* (1990); Chang *et al.* (1973); Dargush and Grigoriev (2002)]. Thus accurate calculation of the domain integrals is important for the successful implementation of the pseudo-initial condition method.

Various methods within the scope of BEM have been proposed to cope with such problem. Sharp [Sharp (1986)] investigated that if the time step is chosen to be too small, the accuracy of the approximation deteriorates. And a stability condition was derived to avoid the problem. Peirce *et al.* [Peirce *et al.* (1990)] investigated that the size of the spatial mesh relative to the time step affected the accumulation of errors in the one-step recursion scheme. Thus they introduced a dimensionless meshing parameter whose magnitude governs the performance of the one-step BEM. The main drawback of the two methods is that if the time step is very small, the computational cost is huge according to requirement of these methods. The authors think that the bottleneck is how to accurately calculate the domain integrals which are involved with the time-dependent fundamental solution. So it is time to develop a new method for evaluating the domain integrals accurately and efficiently. This paper presents a new method for the domain integrals. The new method inherits advantages of the Sharp's stability condition and Peirce's dimensionless meshing parameter. Moreover, a new coordinate transformation coupled with a domain cell subdivision technique is introduced to evaluate the domain integrals. Thus the influence of the size of the spatial mesh relative to the time step is weakened. In our method, firstly a coordinate transformation denoted as (α, β) transformation is introduced [Zhang *et al.* (2009)]. The (α, β) coordinate transformation is similar to the polar coordinate transformation. However, its implementation is simpler than that of polar transformation. Furthermore, a domain cell subdivision technique for 2D BEM is proposed considering the position of the source point, the shape of the cell and a dimensionless meshing parameter which is proposed by Peirce *et al.* With the cell subdivision technique, the integration cells are divided into triangular and quadrilateral

patches. And the rapid variations of the integrand are smoothed out by using the (α, β) transformation on triangular patches. Thus the integrands of domain integrals which vary drastically can be accurately calculated by our method even if the time step is very small. Numerical examples are presented to verify our method. Results demonstrate the accuracy and efficiency of our method.

This paper is organized as follows. In section 2, the boundary integral equation and the domain integral are described. Section 3 introduces the (α, β) transformation and the cell subdivision technique. Numerical examples are given in Section 4. The paper ends with conclusions in Section 5.

2. General Description

2.1. The boundary integral equation

In this section, we study boundary integral solutions to the diffusion equation

$$\nabla^2 u(x, t) - \frac{1}{k} \frac{\partial u(x, t)}{\partial t} = 0 \quad (1)$$

The boundary integral equation for transient heat conduction in an isotropic, homogeneous medium Ω bounded by Γ is given by:

$$\begin{aligned} c(\xi)u(\xi, t_F) + k \int_{t_0}^{t_F} \int_{\Gamma} u(x, t) q^*(\xi, x, t_F, t) d\Gamma(x) dt \\ = k \int_{t_0}^{t_F} \int_{\Gamma} q(x, t) u^*(\xi, x, t_F, t) d\Gamma(x) dt + \int_{\Omega} u_0(x, t_0) u^*(\xi, x, t_F, t_0) d\Omega(x) \end{aligned} \quad (2)$$

where ξ and x are the source point and the field point, respectively. $c(\xi)$ is a function of the internal angle of the boundary at point ξ . k denotes the diffusion coefficient. t_0 and t_F stand for the initial time and the end time of one step, respectively. t represents the time between t_0 and t_F . u^* and q^* are the time-dependent fundamental solution and its derivative with respect to the unit outward normal at the boundary. u_0 is the initial temperature.

The time-dependent fundamental solution u^* in the domain integral is as follows:

$$u^* = \frac{1}{4\pi k \tau} \exp\left(-\frac{r^2}{4k\tau}\right) \quad (3)$$

where r represents the distance between the source point and the field point. τ is the time step, as follows:

$$\tau = t_F - t_0 \quad (4)$$

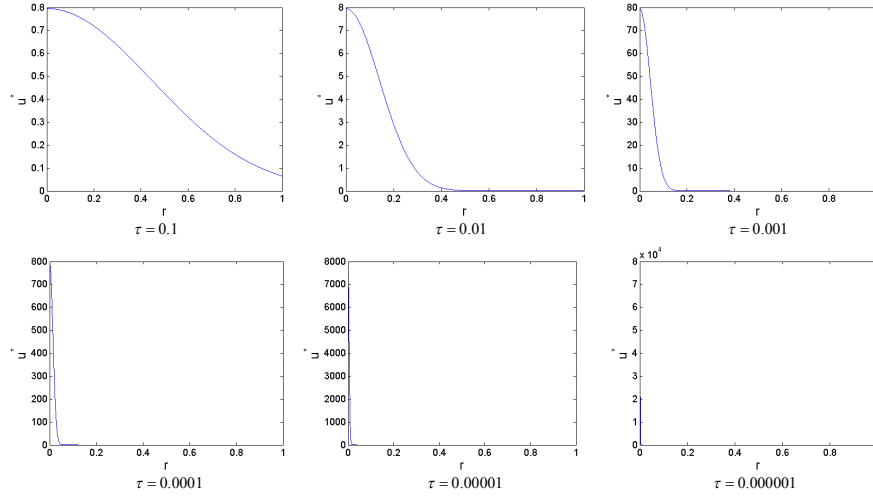


Fig. 1. Variation of u^* with r for several values of time steps.

2.2. The domain integral

The domain integral involved in Eq. (2) is as follows:

$$I = \int_{\Omega} u_0(x, t_0) u^*(\xi, x, t_F, t_0) d\Omega(x) = \int_{\Omega} \frac{u_0(x, t_0)}{4\pi k\tau} \exp\left(-\frac{r^2}{4k\tau}\right) d\Omega(x) \quad (5)$$

The initial temperature $u_0(x, t_0)$ is a regular function. As the time step approaches zero, the integrand in the domain integral (the time-dependent fundamental solution u^*) is close to singular as shown in Fig. 1. Thus the domain integrals can not be accurately calculated by the standard Gaussian quadrature when small time step is used.

3. New Method for Evaluating the Domain Integrals

3.1. The (α, β) transformation

In this section, we first introduce the (α, β) transformation. The transformation can make the integrand in the domain integral more smooth when small time step is used. To construct the (α, β) coordinate system as shown in Fig. 2, the following mapping is used.

$$\begin{cases} x_a = x_0 + (x_1 - x_0)\alpha \\ y_a = y_0 + (y_1 - y_0)\alpha \end{cases} \quad (6a)$$

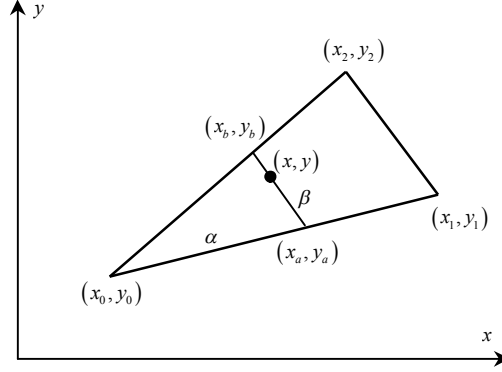


Fig. 2. The (α, β) coordinate transformation.

$$\begin{cases} x_b = x_0 + (x_2 - x_0)\alpha \\ y_b = y_0 + (y_2 - y_0)\alpha \end{cases} \quad (6b)$$

$$\begin{cases} x = x_a + (x_b - x_a)\beta \\ y = y_a + (y_b - y_a)\beta \end{cases} \quad \alpha, \beta \in [0, 1] \quad (6c)$$

where (x_0, y_0) is the source point. And α , β are parameters. The triangle in Fig. 2 is an integration cell or integration patch which is constructed by the cell subdivision technique.

Combining Eqs. (6a)-(6c), the expression for obtaining coordinates x and y can be written as:

$$\begin{cases} x = x_0 + (x_1 - x_0)\alpha + (x_2 - x_1)\alpha\beta \\ y = y_0 + (y_1 - y_0)\alpha + (y_2 - y_1)\alpha\beta \end{cases} \quad (7)$$

The Jacobian of the transformation from the (x, y) system to the (α, β) system is αS_Δ , where

$$S_\Delta = |x_0y_1 + x_1y_2 + x_2y_0 - x_0y_2 - x_1y_0 - x_2y_1| \quad (8)$$

and S_Δ keeps constant over the triangle.

From Eqs. (6a)-(7), it can be noted that the new coordinate system is much simpler to implement than the polar coordinate system. This is due to the fact that both α and β are constrained to the interval $[0, 1]$ in each triangle, thus there is no need to calculate their spans. With the (α, β) transformation, the rapid variations of the integrand are smoothed out in some degree. Thus, the computational accuracy of the domain integrals can be improved.

3.2. The cell subdivision technique

To further improve the computational accuracy of the domain integrals, a cell subdivision technique is proposed in this part. From the Fig.1, it can be seen that a large spike occurs in the integrand near the source point as the time step value is small. Thus the steep slopes produced by the integrand require that integration points be shifted towards the source point in order to evaluate more accurately the integral under consideration. The detailed analysis is as follows.

Firstly we take a derivative of the time-dependent fundamental solution with respect to distance r and the following equation can be obtained:

$$Q(r) = \frac{\partial u^*}{\partial r} = -\frac{r}{8\pi k^2 \tau^2} \exp\left(-\frac{r^2}{4k\tau}\right) \quad (9)$$

Then a dimensionless parameter λ is introduced:

$$\lambda = \frac{l}{\sqrt{k\tau}} \quad (10)$$

when $r = l$, the change rate of the time-dependent fundamental solution with respect to distance r is

$$|Q(l)| = \frac{\exp\left(-\frac{\lambda^2}{4}\right)}{\pi k^{\frac{3}{2}} \tau^{\frac{3}{2}}} \quad (11)$$

Assume $k = 1$, $\tau = 0.001$, when $\lambda > 8$

$$\begin{aligned} l &> 0.2530 \\ |Q(l)| &< 0.0011 \end{aligned} \quad (12)$$

From Eq. (12), when $r = l = 8\sqrt{k\tau}$, the change rate is already very small.

When using the high order cell or discontinuous cell, the positions of the source points ξ shown in Fig. 3 are considered. If the integration cell is subdivided directly into sub-triangles as shown in Fig. 3, the shapes of sub-triangles are poor especially for slender cells, and the numerical results will become less accurate [Xie *et al.* (2013); Qin *et al.* (2011)]. Moreover, from the previous analysis, the rapid variations of the integrand mainly concentrate around the source point. So we need to circumvent the unsmooth region on which the (α, β) transformation is employed and the straightforward Gaussian quadrature is applied on the remaining regions. In order to achieve our goal, the following cell subdivision technique is introduced as shown in Fig. 4:

- (1) Firstly, a square region with the length of $2l$ is constructed to well cover the source point. If the square region beyond the boundary of the cell (the blue dotted line in the Fig. 4), taking that of the cell as the boundary of the square region.
- (2) Secondly, sub-triangles are constructed in square region considering the position of the source point and sub-quadrangles are created in the cell's remaining regions.

There are two advantages of the proposed cell subdivision technique. The first is that the sub-triangles in the proposed method have better shape than that in conventional subdivision method, which is beneficial for the (α, β) transformation to obtain more accurate results. The second is that more integration points are shifted towards the source point and a large number of integration points are avoided. Using the proposed cell subdivision technique coupled with the (α, β) transformation, the domain integrals can be accurately calculated.

4. Numerical Examples

To verify the accuracy and efficiency of our method, several examples are presented in this section. The domain integrals of the following form are considered:

$$I = \int_{\Omega} \frac{1}{4\pi k\tau} \exp\left(-\frac{r^2}{4k\tau}\right) d\Omega \quad (13)$$

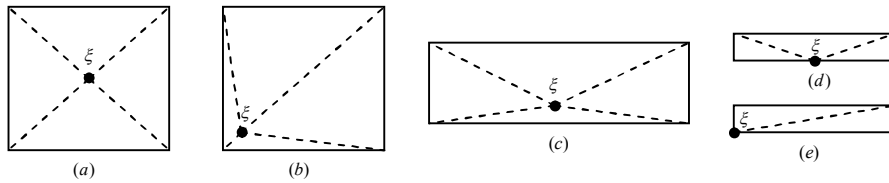


Fig. 3. The conventional subdivisions of quadrilateral cell.

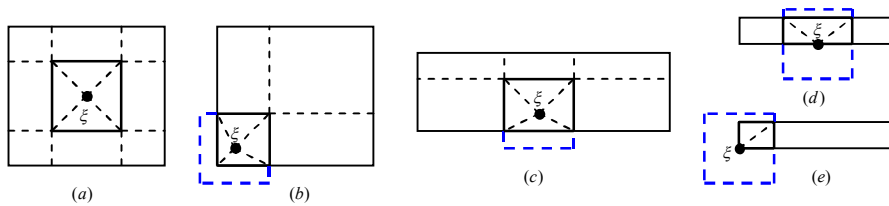


Fig. 4. The new subdivisions of quadrilateral cell.

The coefficient k in Eq. (13) is assumed to be 1 and the dimensionless parameter λ is 8. The (α, β) transformation with 12×12 Gaussian points is used on the sub-triangles and 5×5 point Gaussian quadrature is used on the sub-quadrangles.

The numerical values obtained by our method will be compared to 'exact' values in terms of the relative error defined by

$$\text{Relative Error} = \left| \frac{I_{\text{numerical}} - I_{\text{exact}}}{I_{\text{exact}}} \right| \quad (14)$$

where $I_{\text{numerical}}$ and I_{exact} are the numerical and ‘exact’ values of the integral under consideration, respectively.

4.1. Example 1

In the first example, the domain integral of Eq. (13) is evaluated over a quadrilateral cell with the node coordinates of (0, 0), (1, 0), (1, 1), (0, 1) as shown in Fig. 5. The coordinate of the source point is set at (0.5, 0.5). The relative errors of various methods with different time steps are compared in Table 1. τ represents the time step value. 5×5 means straightforward Gaussian quadrature with 5×5 Gaussian points and the (α, β) transformation combined with the cell subdivision technique is denoted as (α, β) .

Table 1. Relative errors for integral I on quadrilateral cell with the node coordinates of (0, 0), (1, 0), (1, 1), (0, 1). Errors less than 1×10^{-13} are indicated with a ‘-’.

τ	0.1	0.01	0.001	0.0001	0.00001
5×5	2.1323e-06	5.5239e-02	<i>error</i>	<i>error</i>	<i>error</i>
8×8	2.4326e-11	5.1359e-04	<i>error</i>	<i>error</i>	<i>error</i>
10×10	-	1.2984e-05	0.5646	<i>error</i>	<i>error</i>
20×20	-	-	5.6773e-03	<i>error</i>	<i>error</i>
(α, β)	-	1.0307e-10	3.5280e-08	1.0646e-09	9.4669e-10

A number of interesting points can be drawn from Table 1:

- (1) As the time step is large, accurate numerical results can be obtained by applying Gaussian quadrature straightforward, and better accuracy can be obtained with more Gaussian points.
- (2) The standard Gaussian quadrature becomes inefficient and inaccurate to evaluate the domain integral when the time step is smaller than 0.001.
- (3) Using the proposed method, the domain integral can be accurately and efficiently calculated within a wide range of the time step τ .

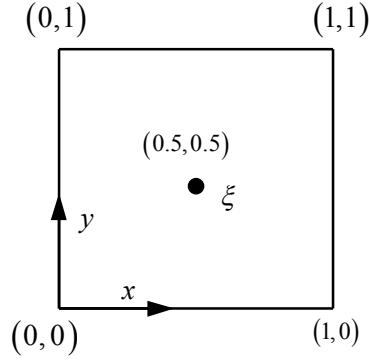


Fig. 5. The node coordinates of quadrilateral cell.

As is illustrated in this example, when the time step is very small, the domain integrals can not be accurately calculated by the standard Gaussian quadrature. However, with our method, high computational accuracy can be obtained within a wide range of the time step τ .

4.2. Example 2

In this example, the above quadrilateral cell shown in Fig. 5 is also considered here. The coordinate of the source point is also set at $(0.5, 0.5)$. In order to verify the importance of the proposed cell subdivision technique, we evaluate the integral of Eq. (13) in two different schemes. The relative errors of the two schemes with different time steps are compared in Table 2. $\text{NDivd}(\alpha, \beta)$ denotes the numerical results obtained by the (α, β) transformation only and $\text{Divd}(\alpha, \beta)$ means the numerical results obtained by the (α, β) transformation in combination with the cell subdivision technique.

Table 2. Relative errors for integral I in two different schemes on quadrilateral cell with the node coordinates of $(0, 0), (1, 0), (1, 1), (0, 1)$. Errors less than 1×10^{-13} are indicated with a ‘-’.

τ	0.1	0.01	0.001	0.0001	0.00001
Exact value	0.54235495	0.99918626	1.00000000	1.00000000	1.00000000
$\text{NDivd}(\alpha, \beta)$	-	1.0307e-10	1.1183e-04	2.3711e-02	0.7252
$\text{Divd}(\alpha, \beta)$	-	1.0307e-10	3.5280e-08	1.0646e-09	9.4669e-10

It can be seen from Table 2 that the results obtained by the combined method are more accurate than those of only (α, β) transformation. More accurate results can be

obtained with the cell subdivision technique when the time step is very small. Thus the cell subdivision technique is necessary to improve the accuracy of the results.

4.3. Example 3

In this example, different locations of the source points on the above quadrilateral cell (Fig. 5) are considered. When using the high order cell or discontinuous cell, the following positions of the source points are concerned. The (α, β) coordinate system and polar coordinate system are used for all cases. (α, β) represents (α, β) transformation combined with the cell subdivision technique and (ρ, θ) denotes polar transformation combined with the cell subdivision technique, respectively. The relative errors of various methods with different time steps are compared in Table 3 and Table 4.

Table 3 and Table 4 show good results can be obtained by the method based on (α, β) transformation considering the different positions of the source points. And the proposed method is not sensitive to the position of the source point. Moreover, it can be found that the accuracy of the method based on polar transformation is lower than that of the proposed method in Table 4. The reason may be that the source points in Table 4 are near to the edge of the cell and the sub-triangles have an irregular shape. Thus (α, β) transformation is more effective than the polar transformation.

Table 3. Relative errors for integral I with different positions of the source points on quadrilateral cell with the node coordinates of $(0, 0)$, $(1, 0)$, $(1, 1)$, $(0, 1)$. Errors less than 1×10^{-13} are indicated with a '-'.²

(α, β)					
τ	0.1	0.01	0.001	0.0001	0.00001
$(0.5, 0.5)$	-	1.0307e-10	3.5280e-08	1.0646e-09	9.4669e-10
$(0.5, 0)$	-	3.4240e-09	1.6660e-08	1.5148e-09	1.4696e-09
$(0, 0)$	-	3.2841e-08	5.1008e-09	1.9926e-09	1.9926e-09
(ρ, θ)					
τ	0.1	0.01	0.001	0.0001	0.00001
$(0.5, 0.5)$	-	1.4539e-11	3.6326e-08	2.1102e-09	1.9922e-09
$(0.5, 0)$	4.0724e-12	3.4238e-09	1.7183e-08	2.0376e-09	1.9924e-09
$(0, 0)$	-	3.2841e-08	5.1008e-09	1.9926e-09	1.9926e-09

Table 4. Relative errors for integral I with the different positions of the source points on quadrilateral cell with the node coordinates of $(0, 0)$, $(1, 0)$, $(1, 1)$, $(0, 1)$. Errors less than 1×10^{-13} are indicated with a '-'.

(α, β)					
τ	0.1	0.01	0.001	0.0001	0.00001
(0.5,0.01)	-	3.5296e-09	3.2219e-06	6.4866e-06	2.1946e-06
(0.02,0.1)	-	1.9436e-08	9.6634e-09	5.5024e-06	1.9621e-08
(0.02,0.01)	-	2.7936e-08	1.2111e-09	6.2566e-09	2.1133e-07
(ρ, θ)					
τ	0.1	0.01	0.001	0.0001	0.00001
(0.5,0.01)	1.4198e-03	1.3448e-03	8.8969e-03	1.0165e-05	3.9739e-08
(0.02,0.1)	7.1337e-04	9.3988e-05	7.2129e-05	1.1805e-06	9.0774e-09
(0.02,0.01)	2.0586e-03	1.7785e-03	4.6845e-04	6.2962e-06	2.1312e-08

4.4. Example 4

To further demonstrate the versatility of the proposed method, the rectangular cells with different length-width ratio are considered as shown in Fig. 6. And source point is located at the center of the cell. a/b is the length-width ratio of the rectangular cell. The relative errors of various methods with different length-width ratio are compared in Table 5.

As shown in Table 5, the accuracy of the proposed method doesn't change with different length-width ratio except for when $\tau = 0.1$. While the accuracy of the method based on polar transformation decreases as length-width ratio becomes large. This demonstrates that the proposed method is more universal than the method based on polar transformation.

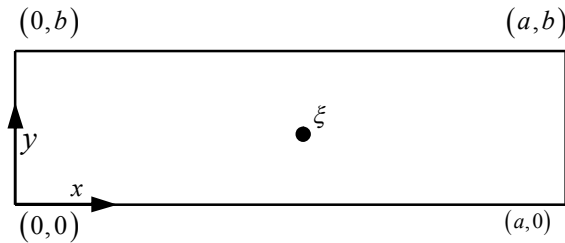


Fig. 6. The node coordinates of rectangular cell.

Table 5. Relative errors for integral I over the rectangular cells with different length-width ratio.

(α, β)					
τ	0.1	0.01	0.001	0.0001	0.00001
$a/b = 2$	1.8529e-13	2.9660e-07	2.0140e-008	1.0056e-09	9.4669e-10
$a/b = 4$	3.2360e-07	3.0342e-07	1.8116e-008	1.0056e-09	9.4670e-10
$a/b = 6$	1.5168e-05	3.1033e-07	1.8113e-008	1.0057e-09	9.4665e-10
$a/b = 8$	1.5168e-05	3.1208e-07	1.8113e-008	1.0056e-09	9.4669e-10
$a/b = 10$	1.5170e-05	3.1239e-07	1.8113e-008	1.0056e-09	9.4666e-10
(ρ, θ)					
τ	0.1	0.01	0.001	0.0001	0.00001
$a/b = 2$	1.6061e-12	3.3554e-09	2.1247e-08	2.1127e-09	2.0538e-09
$a/b = 4$	1.3330e-10	8.4545e-08	9.3619e-08	1.1073e-07	1.1078e-07
$a/b = 6$	1.2535e-08	1.4671e-07	5.1020e-06	5.0849e-06	5.0848e-06
$a/b = 8$	5.1179e-07	2.3291e-06	4.4667e-05	4.4650e-05	4.4650e-05
$a/b = 10$	2.0323e-06	5.5103e-06	1.3158e-04	1.3157e-04	1.3157e-04

4.5. Example 5

A more general example is presented in this example and the domain integral of the following form is considered:

$$I' = \int_{\Omega} (x^2 + y^2) \frac{1}{4\pi k\tau} \exp\left(-\frac{r^2}{4k\tau}\right) d\Omega \quad (15)$$

The domain integral of Eq. (15) is evaluated over a slender rectangular cell with the node coordinates of (0, 0), (10, 0), (10, 1), (0, 1). Source points with different locations are considered. The relative errors with different time steps are compared in Table 6.

From Table 6, good accuracy can be achieved by the proposed method for different cases. For instance, when the coordinate of the source point is set at (5, 0), the max relative error is less than 10^{-6} . This example illustrates our method is effective to calculate the domain integrals even the time step is very small.

Table 6. Relative errors for integral I' over the irregular rectangular cells on the different position of the source points.

τ	0.1	0.01	0.001	0.0001	0.00001
(5,0.1)	7.6612e-06	6.3884e-06	2.1893e-06	1.0983e-08	1.9581e-09
(5,0)	4.0316e-06	2.0538e-08	3.3416e-09	1.4535e-09	1.4680e-09
(0,0.5)	1.8154e-07	5.0096e-08	2.3153e-09	9.0916e-11	1.3086e-09
(0.1,0.5)	1.5293e-07	3.6787e-08	1.8424e-06	9.1308e-09	1.7859e-09
(1,0.5)	8.0928e-08	2.8842e-07	1.6424e-08	6.8424e-10	9.1453e-10
(0, 1)	1.3699e-07	2.0893e-08	1.7121e-08	7.1901e-09	3.6989e-09
(1,0.9)	6.2464e-08	6.3693e-06	2.3670e-06	1.1640e-08	1.9671e-09
(2,0.8)	2.0517e-06	5.5710e-06	1.7826e-08	6.7614e-09	9.3972e-10
(0.2,0.1)	1.6018e-07	1.7957e-07	4.1464e-07	3.6358e-09	1.0562e-09

5. Conclusions

A general algorithm for the evaluation of the domain integrals which appear in 2D boundary element method for transient heat conduction problems was proposed in this paper. Employing the proposed method, the domain integrals can be effectively and accurately calculated. Furthermore, a domain cell subdivision technique takes into account the position of the source point, the shape of the integration cell and the relations between the size of cell and the time step. Thus even the time step is very small, accurate results can still be obtained by our method. Numerical examples were presented to verify our method. Results demonstrated the accuracy and efficiency of our method. Extension of our work to 3D transient BEM is ongoing.

Acknowledgements

This work was supported in part by National Science Foundation of China under grant number 11172098, in part by National 973 Project of China under grant number 2010CB328005 and in part by Hunan Provincial Natural Science Foundation for Creative Research Groups of China (Grant No.12JJ7001).

References

- Xue, B. Y., Wu, S. C., Zhang, W. H. and Liu, G. R. (2013). A smoothed FEM (S-FEM) for heat transfer problems. *Int. J. Comput. Meth.*, **10**: 1340001 (13 pages).

- Hamza-Cherif, S. M., Houmat, A. and Hadjoui, A. (2007). Transient heat conduction in functionally graded materials. *Int. J. Comput. Meth.*, **4**: 603-619.
- Brebbia, C. A., Telles, J. C. F. and Wrobel, L. C. (1984). Boundary element techniques: theory and applications in engineering. Vol. 5. Berlin: Springer-Verlag.
- Sutradhar, Alok, Paulino, G. H. and Gray, L. J. (2002). Transient heat conduction in homogeneous and non-homogeneous materials by the Laplace transform Galerkin boundary element method. *Eng. Anal. Bound. Elem.*, **26**: 119-132.
- Hill, L. R., and Farris, T. N. (1995). Fast fourier transform of spectral boundary elements for transient heat conduction. *Int. J. Numer. Method H.*, **5**: 813-827.
- Ibáñez, M. T. and Power, H. (2000). An efficient direct BEM numerical scheme for heat transfer problems using Fourier series. *Int. J. Numer. Method H.*, **10**: 687-720.
- Gupta, A., Jr, J. M. S. and Delgado, H. E. (1995). An efficient bem solution for three-dimensional transient heat conduction. *Int. J. Numer. Method H.*, **5**: 327-340.
- Ma, F., et al. (2008). Transient heat conduction analysis of 3D solids with fiber inclusions using the boundary element method. *Int. J. Numer. Meth. Eng.*, **73**: 1113-1136.
- Wang, C. H., Grigoriev, M. M. and Dargush, G. F. (2005). A fast multi-level convolution boundary element method for transient diffusion problems. *Int. J. Numer. Meth. Eng.*, **62**: 1895-1926.
- Zhou, F., et al. (2013). Transient heat conduction analysis of solids with small open-ended tubular cavities by boundary face method. *Eng. Anal. Bound. Elem.*, **37**: 542-550.
- Lesnic, D. (2004). The determination of the unknown thermal properties of homogeneous heat conductors. *Int. J. Comput. Meth.*, **1**: 431-443.
- Mukherjee, S., and Liu, Y. J. (2013). The boundary element method. *Int. J. Comput. Meth.*, **10**: 1350037 (91 pages).
- Zhuang, C., et al. (2012). Integration of subdivision method into boundary element analysis. *Int. J. Comput. Meth.*, **9**: 1240019 (11 pages).
- Dargush, G. F., and Banerjee, P. K. (1991). Application of the boundary element method to transient heat conduction. *Int. J. Numer. Meth. Eng.*, **31**: 1231-1247.
- Guo, S., et al. (2013). Three-dimensional transient heat conduction analysis by Laplace transformation and multiple reciprocity boundary face method. *Eng. Anal. Bound. Elem.*, **37**: 15-22.
- Sharp, S. (1986). Stability analysis for boundary element methods for the diffusion equation. *Appl. Math. Model.*, **10**: 41-48.
- Peirce, A. P., Askar, A. and Rabitz, H. (1990). Convergence properties of a class of boundary element approximations to linear diffusion problems with localized nonlinear reactions. *Numer. Meth. Part. D. E.*, **6**: 75-108.
- Chang, Y. P., Kang, C. S. and Chen, D. J. (1973). The use of fundamental Green's functions for the solution of problems of heat conduction in anisotropic media. *Int. J. Heat Mass Tran.*, **16**: 1905-1918.
- Dargush, G. F., and Grigoriev, M. M. (2002). Higher-order boundary element methods for transient diffusion problems. Part II: Singular flux formulation. *Int. J. Numer. Meth. Eng.*, **55**: 41-54.
- Zhang, J., et al. (2009). A boundary face method for potential problems in three dimensions. *Int. J. Numer. Meth. Eng.*, **80**: 320-337.
- Xie, G., et al. (2013). New variable transformations for evaluating nearly singular integrals in 3D boundary element method. *Eng. Anal. Bound. Elem.*, **37**: 1169-1178.
- Qin, X., et al. (2011). A general algorithm for the numerical evaluation of nearly singular integrals on 3D boundary element. *J. Comput. Appl. Math.*, **235**: 4174-4186.